A fundamental study on velocity restoration for tidal farm

A. D. Hoang[1] · C. J. Yang[†]

Abstract: With the worldwide trend of controlling the utilization of fossil fuels inducing global climate change, many efforts will have to be made on securing a sustainable energy supply. Tidal current is a concentrated form of gravitational energy, its resource is significant, but limited locations. To effectively capture tidal current energy from the sea, a group of tidal turbines should be formed and positioned with optimal size and spacing for absorbing from multiple points. Thus, the flow field including turbines becomes a huge domain, a so-called tidal farm. It can be very convenient technically and economically if a whole turbine farm is simulated by means of actuator disc thoery. So, the analysis method using actuator discs coupled with a solution of Reynolds Averaged Navier-Stokes (RANS) equations is adopted for actual tidal turbines. Actuator discs have regions where similar forces imposed by actual turbines are applied to a flow. As working in group formation, turbines naturally have interaction effects on one another. Therefore, the present paper investigate the evaluation on the operating performance of tidal farm in terms of the mutual influence among turbine units with various lateral and longitudinal spacing. Authors expect that results of the present study contribute to the development of tidal farm for the future potential energy.

Keywords: Tidal farm, CFD, Actuator disc, Tidal energy, Velocity restoration.

Nomenclature

a : induction factor

A_d : disc area (m2)

C_T : thrust coefficient

C_P : power coefficient

D: turbine disc diameter (m)

K : resistance coefficient

S_i : momentum source

T : thrust (N)

U : water velocity (m/s)

U_o : inflow velocity (m/s)

U_d : velocity at disc (m/s)

x : lateral distance (m)

y : longitudinal distance (m)

ρ : density

μ : viscosity

$-\overline{\rho u_i' u_j'}$: Reynolds stress

1. Introduction

The ocean, covering 70% of the Earth's surface, produces a vast amount of kinetic energy in the form of tides and waves. With the increasing prices for fossil fuels, a growing demand for electricity worldwide, and increased concern with global warming caused by carbon emissions as mentioned above, ocean energy may soon find a place in the energy marketplace. Few studies have been carried out to de-

† Corresponding author: Division of Marine Engineering, Mokpo National Maritime University, 91 Haeyangdaehak-ro, Mokpo-si, Jeollanam-do 530-729, Republic of Korea, E-mail: cjyang@mmu.ac.kr, Tel: 061-240-7228

1 Division of Marine Engineering, Graduate School, Mokpo National Maritime University, E-mail: had@mmu.ac.kr, Tel: 061-240-7242

termine the total global marine current resource, although it is estimated to exceed 450 GW [1]. Locations with especially intense currents are found around the British Islands and Ireland, between the Channel Islands and France, in the Straits of Messina between Italy and Sicily and in various channels between the Greek Islands in the Aegean. Other large marine current resources can be found in regions such as South East Asia together with Japan and Korea, both the east and west coasts of Canada and certainly in many other places around the globe that require further investigation.

Tidal turbines are much like submerged windmills. They are optimally located in the sea where there are high tidal current velocities; the huge volumes of flowing water turn the blades of the turbines, thereby producing electricity. Unlike wind, these turbines have the major advantage of predictability: not only are tides far more constant than wind, but tidal patterns can also be calculated years in advance. Thus, it is possible to form a tidal turbine farm formation like wind energy farm; hence tidal power can be captured in large area at multiple points simultaneously.

Therefore, tidal farm is the interest of present paper, where research is conducted to evaluate the turbines' energy absorption rate as well as the rate of restoration of water kinetic energy evaluate the rate of energy absorption of turbines as well as the rate of restoration of water kinetic energy. As working in arrays, turbines naturally have interaction among them. Previous studies have investigated on this interaction for different longitudinal spacing between turbines [2][3]. Therefore, this paper continues author's study aimed for two objectives: to estimate tidal turbines performance at different lateral spacing and to evaluate performance of a given staggered tidal farm which consists of seven turbine units.

2. Numerical Methods

2.1 Actuator disc theory

Albert Betz (1885 - 1968), a German physicist and a pioneer of wind turbine technology, introduced a method to determine the limit power of extraction in a fluid. That is the "Actuator Disc Theory", the method [3] for characterization of an actual tidal turbine in a solution of Reynolds-averaged Navier-Stokes equations. The application of the model in an infinite volume of air is used in the analysis and design of wind turbines. Since the flow of air in the atmosphere is different to that of a liquid constrained in an open channel due to the air's negligible density, actuator disc theory can be applied for tidal turbines with some modification and extra consideration. Actuator disc play an important role in study of multi turbine array. Thus, the flow field including turbines becomes a huge domain, a so-called tidal farm. It can be very convenient technically and economically if a whole turbine farm is simulated by means of actuator disc theory.

The true fluid flow passing around and through a tidal turbine is governed by the Reynolds-averaged Navier-Stokes (RANS) equations. They are time-averaged equations of motion for fluid flow. Thus, combining the law of conservation of mass with the transport theorem yields the continuity equation and is written as:

$$\frac{\partial U_i}{\partial x_i} = 0 \qquad (1)$$

The momentum equation expresses Newton's second law of motion for a fluid flowing through a finite control volume. This study is steady state analysis, so the equation is:

$$\frac{\partial(\rho U_i U_j)}{\partial x_j} = -\frac{\partial p}{\partial x_i} +$$
$$+ \frac{\partial}{\partial x_j}\left[\mu\left(\frac{\partial U_i}{\partial x_j} + \frac{\partial U_j}{\partial x_i}\right)\right]$$
$$+ \frac{\partial}{\partial x_j}\left(-\rho\overline{u_i' u_j'}\right) + \rho g_i + S_i \qquad (2)$$

Reynolds stress $-\rho\overline{u_i' u_j}$ is resolved by turbulence model. S_i represents the immersing effect of turbine at disc region and is calculated as follow:

$$S_i = \frac{K}{\Delta x}\frac{\rho}{2} U_{i(d)}\left| U_{i(d)} \right| \qquad (3)$$
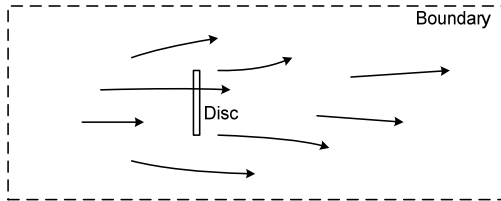

Figure 1: Actuator disc demonstration

Resistance coefficient of turbine is found to be 2 for most practical case **[4]**. K = 0 corresponds to free flow state, or no turbine is submerged into the stream. K = 4 corresponds to break-state, meaning turbine is unable to rotate or no water passes through the disc.

The actuator disc is applied a constant resistance to the incoming flow. This resistance causes a thrust to be imposed on the flow and this thrust should be similar to that imposed by the turbine simulated. For a turbine, thrust will vary based on the incoming flow, geometry, pitch of the blades, and rotational speed. For an actuator disc, thrust depends on its resistance coefficient and the inflow velocity, this is shown as:

$$T_i = K\frac{\rho}{2} U_{i(d)}\left| U_{i(d)} \right| A_d \qquad (4)$$

The turbine is then typically characterized in terms of its thrust coefficient, which is defined as:

$$C_T = \frac{T}{\frac{1}{2}\rho U_0^2 A_d} \qquad (5)$$

By characterizing an actuator disc with a given C_T which features a real turbine's characteristic, the disc becomes a represented tidal turbine. Therefore, results from actuator disc simulation can be used to evaluate real turbine's performance with acceptable accuracy **[2]**.

2.2 Calculation conditions

Initial input parameters are listed in **Table 1**. This calculation domain is made for a scale scenario with Froude number, Fr = 0.175. Thus, it is corresponded to an actual model of 10m turbine in a 30m water depth channel with mean inflow velocity of 3m/s. Typical value of Froude number for full scale channels are within 0.1 - 0.2, and value less than 0.5 generally ensure stable flow when there are no obstacles in water column **[5]**.

Boundary conditions are as follows:

Inlet: Cartesian normal speed. Since the flow is affected by seabed surface roughness, the velocity has gradient characteristic as defined by 1/10th power law. Initial water level is set to 0.3m.

Outlet: Static pressure.

Sidewall: Free slip wall boundary.

Bed plane: As real sea bed is rough surface. So nonslip wall is defined for this boundary.

Disc front and rear walls: Free slip walls with flux sources.

Disc cylinder: Free slip wall.

Free surface: Volume of fluid model **[6][7]**.

Simulation using ANSYS CFX **[8]** is done in steady state. Turbulence model k-ε is used since it is the most commonly used of all the turbulence models in CFD **[9]**. For steady state calculations, max integration is set to 4,000 to ensure convergence with convergence criteria of 1×10^{-5}.

The axial induction (sometimes called interference) factor, a, is defined as the fractional decrease in wind velocity between the free stream (upwind) and the rotor plane:

$$a = 1 - \frac{U_d}{U_0} \qquad (6)$$

As a increases from zero, the downwind flow speed steadily decreases until, a = 1/2, meaning that the rotor has completely stopped and the simple theory is no longer applicable. According to Betz theory, turbine reaches maximum power efficiency at a = 1/3, corresponds to C_T = 0.89 **[10]**.

Table 1 Initial calculation conditions

Parameters	Values
Domain size	8m(L)×1m(W)×0.5m(H)
Disc diameter	0.1m
Disc thickness	0.004m
Froude number	0.175
Reynolds number	3.5×10^4
Inflow velocity	$U_0 = 0.3 \left(\dfrac{y}{0.15} \right)^{\frac{1}{10}}$ (m/s)
Induction factor	a = 1/3
Thrust coefficient	C_T = 0.89

3. Results and Discussions

3.1 Lateral turbine array

The previous section stated that the longitudinal spacing has major influence to turbine. Turbines in tidal farm are also positioned laterally, so the influence of lateral spacing should as well be evaluated. However, since the lateral array turbines do not share the same inline stream, the lateral spacing is much shorter than longitudinal spacing. Lateral spacing is set just to avoid disturbance effect of turbines due to their downstream wakes.

The calculation domain for lateral positioned turbine array adopted hexa mesh style which consists of one million nodes (**Figure 2**). The domain is shown in **Figure 3**. Simulation is done for three cases corresponding to three different lateral spacings: 2.0D, 2.5D and 3.0D. Domain size is 8m(L)×1m(W)×0.5m(H) which is large enough to position three discs inline along the width in all cases.
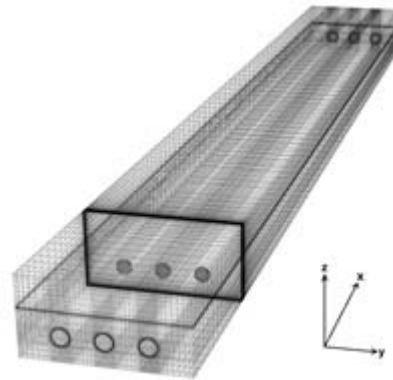

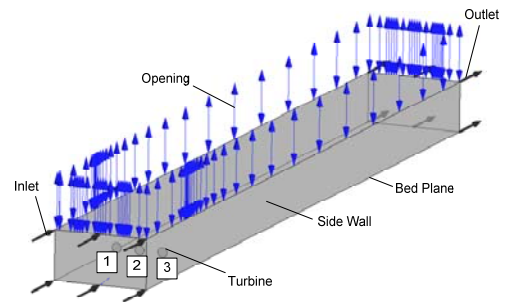**Figure 2:** Mesh formation of lateral array

Figure 3: Calculation domain of lateral array

In this simulation, turbines are numbered No. 1, No. 2 and No. 3 from left to right as marked in **Figure 3**.

Flow visualization in horizontal view (XY plane) is shown in **Figure 4**. According to the flow pattern, three cases show the similar velocity contours of water and air. In 3D lateral spacing case, there is a small fluctuation of air velocity at inlet, but this is not considered as an influence to the turbine group's performance since there is no abnormal variation in water velocity. These contours generally present the flow pattern in term of visualization.

Figure 5 shows the velocity deficit along the centerline of turbines at different lateral spacings. For 2D lateral spacing, turbine No. 2 obtains the highest power coefficient, C_{P2} = 49.48%, the two remaining have the same lower value, $C_{P1} = C_{P3}$ = 49.23%. Since turbine No. 2 absorbed more power, its restora
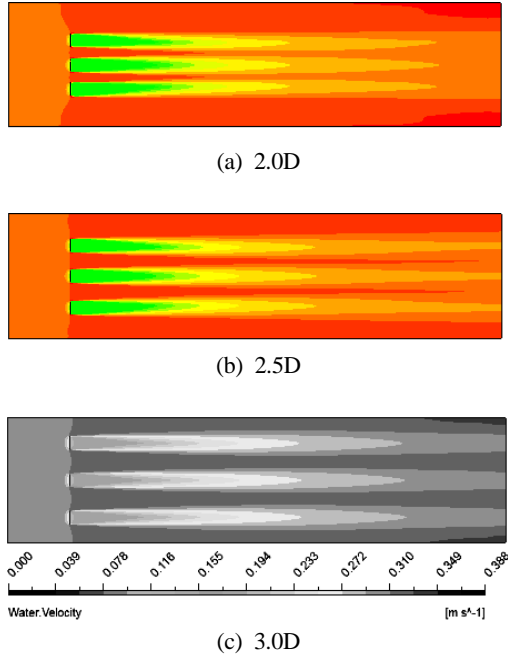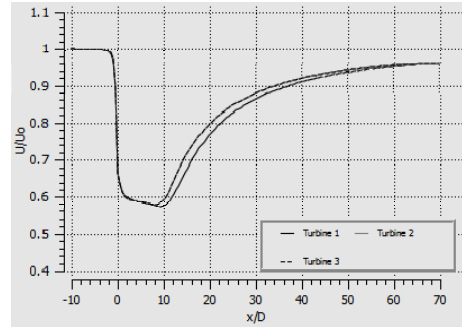
(a) 2.0D

(b) 2.5D

(c) 3.0D

Figure 4: Flow visualization of lateral array

(a) 2.0D

(b) 2.5D

(c) 3.0D

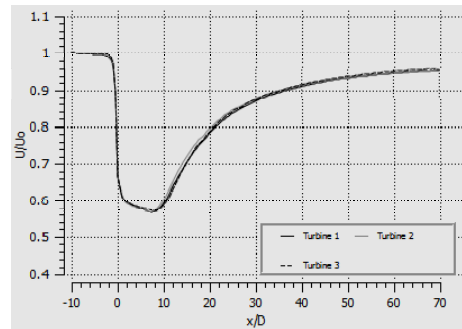**Figure 5:** Deficit along the centerline in lateral array

tion is slower than the rest (Fig. 5a), but all of them show the similar restoration characteristic at far wake location, from 60D to 70D. Maximum restoration reaches 96% at 70D downstream location.

When the lateral spacing is increased to 2.5D, the three turbines get their power coefficients C_{P1} = 49.25%, C_{P2} = 49.48% and C_{P3} = 49.33%, respectively. The difference in power efficiency is relatively reduced but clarified deficit of the three turbines is still visible in Fig. 5b. The restoration of the three is almost the same and also reaches 96% at 70D.
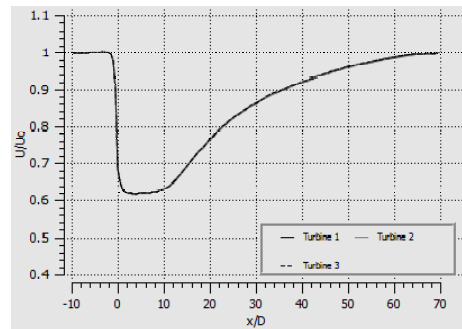
When the lateral spacing is increased to 3D, all three turbines almost have the same deficit curve. Their power coefficients all reach 49.48%.Thus, these results show that 3D lateral spacing is wide enough to minimum mutual influence between the lateral array turbines. And in this arrangement, fully restoration is visible at 70D downstream location. But in fact, it is uneconomical to arrange turbine array with longitudinal spacing up to 70D. Instead, the range

from 20D to 30D in previous study is claimed to be long enough for longitudinal spacing, with thin this value high restoration rate of about 80-90% is available and acceptable. Therefore, more spacing is saved for other arrays.

Thus, according to these results, all cases are selectable since the lateral influence is not as considerable as compared to longitudinal case. 3D is found

to be the optimum lateral spacing in current study but 2.0D will be more advantageous in narrow channels.

3.2 Staggered turbine array

Staggered formation is a well known formation in which elements are at different levels and are not abreast of each other. This is to ensure the safe interaction among elements in some group operation. Staggered formation can be applied to tidal turbine farm and it is claimed as an effective formation for the longterm stable operation of tidal turbines.

Previous study has shown that 3D lateral spacing and 20D-35D longitudinal spacing are enough to ensure the stable operation of turbines and minimum the disturbance effects between them [2]. Thus, these settings are applied in staggered formation simulation. In detail, the number of turbine is chosen to be seven, they will be spaced 30D longitudinally and 3D laterally. The turbine group is positioned in staggered formation as shown in Fig. 6 which shows the calculation domain; turbines are numbered from 1 to 7. **Figure 7** shows the mesh formation for this domain. The mesh contains 1 million nodes, is sized 5.5m(L) × 1.5m(W) × 0.5m(H) and is large enough in order to simulate seven turbines in the same flow field. Initial parameters are maintained the same as lateral array simulation.
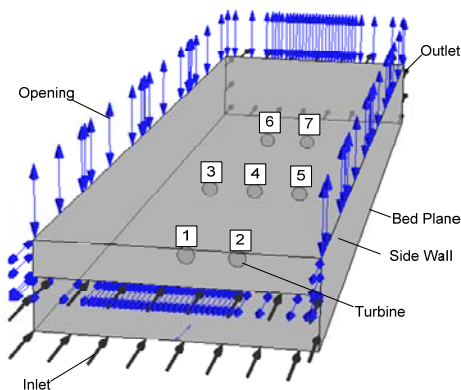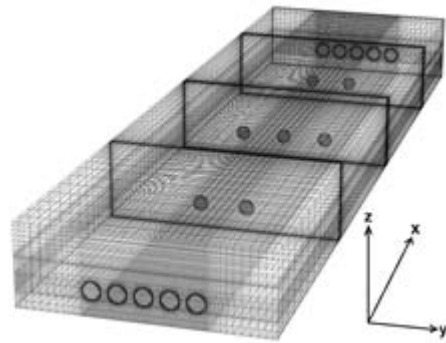

Figure 7: Staggered formation domain

Figure 8 presents the flow pattern at horizontal center plane (ZX plane). Since all the turbines are properly placed and positioned, there is no presence of any abnormal flow or disturbance among their streams. The color contour shows uniform variation of velocity at each turbine unit. There is a notice that the outlet boundary condition is set at a relative longitudinal spacing of 30D downstream location for the two on last row (No. 6 and No. 7 turbine). Thus, the far end at these turbines is a little influenced by outlet boundary condition so that their continuity of velocity variations are not maintained as normally shown for the inline upstream turbines.
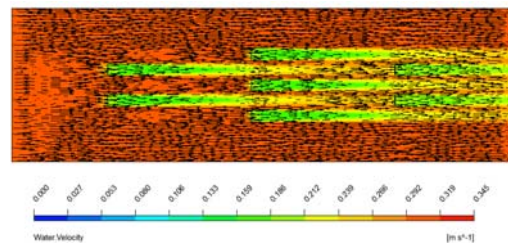

Figure 8: Velocity vector field in staggered formation

Velocity deficit of each turbine unit is shown in **Figure 9**. Resulted from calculation data, maximum power coefficient is found at turbine No. 4, $C_{P4} = 53.92\%$, the other unit in second row also get high power efficiency, $C_{P3} = 53.58\%$ and $C_{P5} = 53.56\%$.

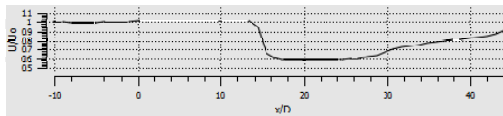**Figure 6:** Calculation domain of staggered formation domain

The first row has lower power coefficient, $C_{P1} = 47.5\%$, $C_{P2} = 47.5\%$ and the last row has the lowest efficiency, $C_{P6} = C_{P7} = 30.36\%$.
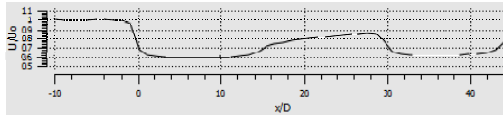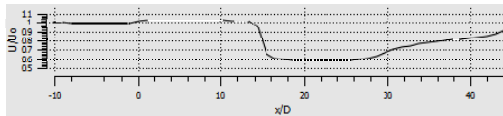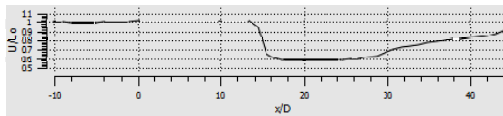

(a) Turbine No.1 & No.6
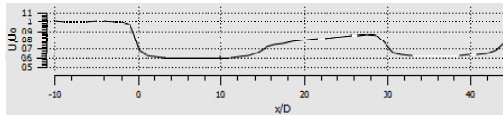
(b) Turbine No.2 & No.7

(c) Turbine No.3

(d) Turbine No.4

(e) Turbine No.5

Figure 9: Deficit along the centerline in staggered formation

Turbines at the first row are the first to contact the stream, thus their power absorption rates are exactly the same. They also have similar velocity deficit curves (**Figure 9a** and **9b**). This exists in the second and third rows as well but it is not a complete similarity. Because disturbance should have effect after the first row's encounter, turbines at the second row have relatively different outcomes. Even the smallest mutual influence can lead to these differences. Maximum could not be obtained at the first row since it is closer to the inlet in comparison with the second row. Therefore, inflow velocity is not yet fully developed as the flow entered the first row of turbine. Velocity restoration rate ranged from 0.8 to 0.93 in actuator disc based simulation. Turbines in the second rows have the highest restoration rate. This is clearly understandable since they are positioned individually in longitudinal array, besides; these turbines have longer downstream distance for restoration.

4. Conclusions

The tidal energy conversion technologies in a good tidal site can provide a cost of electricity in the similar range as existing commercial wind technologies. This paper introduces velocity interactions based on actuator discs for tidal farm. To summarize the work presented above, we can conclude as follows.

1) Power coefficient is inversely proportional to the restoration rate. The higher power turbine disc absorbed, the longer restoration proceeds.

2) For lateral turbine array, there is an identical influence between turbines. In general, all tested cases are acceptable and wider spacing is preferable but is limited in narrow channel, where 2.0D lateral spacing is more advantageous.

3) Staggered formation is found to be proper formation for tidal farm, it reduce unwanted disturbance influence among turbines without increasing size of the whole flow field.

This study has not yet shown uniform performance of turbine components all over the formation, but it is understandable as the influence among turbines. Hence, future works will be carried out to investigate interactions among turbines with rotor blades.

References

[1] Carbon Trust Hompage, Marine energy http://www.carbontrust.com/resources/reports/technology/marine-energy, Accessed September

28, 2013.

[2] L. Bai, R. R. G. Spence, and G. Dudziak, "Investigation of the influence of array arrangement and spacing on tidal energy converter (TEC) performance using a 3-dimentional CFD model", Proceeding of the 8th European Wave and Tidal Energy Conference, pp. 1-8, 2009.

[3] C. J. Yang, A. D. Hoang, and Y. H. Lee, "An evaluation for predicting the far wake of tidal turbines positioned in array at different longitudinal spaces", Journal of the Korean Society of Marine Engineering, vol. 36, no. 3, pp. 358-367, 2012.

[4] J. Whelan, M. Thomson, J. M. R. Graham, and J. Peiró, Modeling of Free Surface Proximity and Wave-Induced Velocities Around a Horizontal Axis Tidal Stream Turbine, Technical Report CS-TR-12-98, Department of Aeronautics, Imperial College, UK, 2012.

[5] G. T. Houlsby, S. Draper, and M. L. G. Oldfield, Application of Linear Momentum Actuator Disc Theory to Open Channel Flow, University of Oxford, Report No. 2296/08, 2008.

[6] M. E. Harrison, W. M. J. Batten, L. E. Myers, and A. S. Bahaj, "Comparison between CFD simulations and experiments for predicting the far wake of horizontal axis tidal turbines", IET Renew Power Generation, vol. 4, pp. 613-627, 2009.

[7] J. I. Whelan, J. M. R. Graham, and J. Peiró, "A free surface and blockage correction for tidal turbines", Journal of Fluid Mechanics, vol. 624, pp. 281-291, 2009.

[8] ANSYS Incorporated, ANSYS CFX-Solver Theory Guide, 2009.

[9] W. Graebel, Advanced Fluid Mechanics, Academic Press, 2007.

[10] T. Burton, Wind Energy Handbook, John Wiley and Sons Press, 2001.